Disentangling acute motor deficits and adaptive responses evoked by the loss of cerebellar output

Nirvik Sinha[a,b,c], Sharon Israely[a], Ora Ben Harosh[a], Ran Harel[d], Julius PA Dewald[b,c,e,f], Yifat Prut[a]

[a]Edmond and Lily Safra Center for Brain Sciences, The Hebrew University of Jerusalem, 9190401 Jerusalem, Israel; [b]Department of Physical Therapy and Human Movement Sciences, Northwestern University Feinberg School of Medicine, Chicago, IL 60610; [c]Interdepartmental Neuroscience Center, Northwestern University Feinberg School of Medicine, Chicago, IL 60611; [d] Department of Neurosurgery, Sheba Medical Center, 5262000 Tel Aviv, Israel; [e]Department of Biomedical Engineering, Northwestern University, Evanston, IL 60208; [f] Department of Physical Medicine & Rehabilitation, Northwestern University Feinberg School of Medicine, Chicago, IL 60610

*Nirvik Sinha; *Yifat Prut

Email: Nirvik.Sinha@mail.huji.ac.il

yifat.prut@mail.huji.ac.il

Author Contributions: Y.P. designed research; N.S., S.I., O.B.H., and R.H. performed research; N.S. and S.I. analyzed the data; N.S., J.P.A.D., and Y.P. wrote the paper.

Competing Interest Statement: The authors declare no competing interest.

Classification: Major: Biological Sciences, Minor: Neuroscience

Keywords: cerebellum | nonhuman primates | coupling torques | weakness | motor noise

Abstract

Cerebellar patients exhibit a broad range of impairments when performing voluntary movements. However, the sequence of events leading to these deficits and the distinction between primary and compensatory processes remain unclear. We addressed this question by reversibly blocking cerebellar outflow in monkeys performing a planar reaching task. We found that the reduced hand velocity observed under cerebellar block is driven by a combination of a general decrease in muscle torque and a spatially tuned reduction in velocity, particularly pronounced in movements involving inter-joint interactions. The time course of these two processes was examined using repeated movements to the same target under cerebellar block. We found that the reduced velocity was driven by an acute onset of weakness superimposed on a gradually emergent strategy aimed to minimize passive inter-joint interactions. Finally, although the reduced velocity affected movements to all targets, it could not explain the enhanced motor noise observed under cerebellar block, which manifested as decomposed and variable trajectories. Our results suggest that cerebellar deficits lead to motor impairments through a loss of muscle strength and altered motor control strategy to compensate for the impaired control of limb dynamics. However, the loss of feedforward control also leads to increased motor noise, which cannot be strategically eliminated.

Significance Statement

Our study examined the impact of cerebellar dysfunction on motor control by reversibly blocking the cerebellar output in monkeys. Under cerebellar block, movements initially slowed due to acute-onset muscle weakness. Beyond this primary deficit, there was a secondary, seemingly strategic, slowing of movements aimed at mitigating inter-joint interactions associated with rapid, ballistic movements. Finally, during the cerebellar block we observed movement variability increased independently of the reduced velocity, likely reflecting errors in movement planning. Taken together, these findings highlight the role of cerebellar information in motor control and delineate the sequence of processes following cerebellar dysfunction that culminate in a broad range of motor impairments.

Main Text

Introduction

The ability to coordinate well-timed movements greatly relies on the cerebellum as evident from studies of individuals with cerebellar ataxia (1). The cerebellum regulates timing of movements by predicting the mechanical interactions between adjacent joints (2, 3), a computation that requires an internal model of feedforward control (4-10). However, motor deficits exhibited by cerebellar patients extend much beyond poor motor timing, including loss of muscle tone (11-13), sensory deficits (14, 15), etc. Accumulating clinical data collected from cerebellar patients provide conflicting evidence regarding underlying pathophysiology of the loss of cerebellar signals (16-19), most likely due the heterogeneity of individuals with chronic cerebellar deficits, where the primary and secondary effects are inseparable. Therefore, the sequence of events leading to the observed motor impairments in cerebellar patients is still unclear.

To address this question, we trained monkeys to perform a planar reaching task supported by an exoskeleton. Cerebellar output to the motor cortex was reversibly blocked using high-frequency stimulation through the superior cerebellar peduncle (20) and the effect of this manipulation was measured during performed movements. We found that the loss of cerebellar outflow led to reduced hand velocity reflecting two parallel underlying mechanisms. First, there was an overall reduction in muscle torques, even for movement directions where inter-joint interactions were low, thereby reflecting weakness. Second, the reduction in hand velocity exhibited a spatial tuning and was particularly strong for directions which generated large inter-joint interactions, thereby reflecting an inability to compensate for limb dynamics. The time course of these two mechanisms was identified when monkeys performed repeated movements to the same target under cerebellar block. Hand

velocity was low initially, reflecting a primary weakness, and declined further in successive trials, revealing an adaptive motor strategy to minimize inter-joint interactions. Finally, we found that the decrease in velocity during cerebellar block could not fully explain the noisy and decomposed movements observed under these conditions, which may be due to an impaired state estimate of the limb that leads to the faulty feedforward control of inter-joint interactions. Taken together, we show that cerebellar output is essential for generating sufficient muscle torques to allow fast and stereotypical movements while overcoming the complex inter-joint interactions inherent in such actions. The loss of this output triggers a sequence of early primary effects followed by compensatory responses aimed to mitigate these impairments. Together these processes result in significantly slow movements.

Results

Slower movements in cerebellar block are due to weakness and impaired limb dynamics.

We trained 4 adult monkeys (*Macaca fascicularis*) to sit in a primate chair with their upper limb supported by an exoskeleton (KINARM system) and perform a planar center-out reaching task (**Figure 1a, b**). The spatial location of the targets enabled us to dissociate between shoulder-dominant (lateral targets) vs. shoulder-elbow movements (diagonal and straight targets respectively).

Movements exhibited a significant reduction in the peak hand velocity during cerebellar block in a manner that was direction-dependent (2-way ANOVA, effect of cerebellar block: $p = 0.029$, effect of targets: $p < 0.001$, interaction effect: $p = 0.008$; **Supplementary table S1**). Post-hoc comparisons revealed that the effect on targets 1-4 located away from the body was significantly larger than on targets 5-8 located near the body (**Figure 1c**, mean decrease of 8.2%, CI [7.4, 9.1], $p < 0.001$ for targets 1-4 compared to mean decrease of 2.2%, CI [1.2, 3.2], $p < 0.001$ for targets 5-8). In the task used in this study, hand movements were made by controlling the muscle torque at the shoulder and the elbow (21). Under these conditions, simultaneous movements of both joints generated coupling torques due to passive interactions between limb inertial properties and joint velocities (22, 23). These coupling torques could explain the target-specific effect of cerebellar block. We therefore used an inverse dynamics model of the upper limb to identify the target-specific muscle and coupling torques (24). We found that the coupling torque varied in a target-dependent manner during both the control and cerebellar block conditions (**Figure 1d** and **Supplementary table S2**), Specifically, during control, coupling torques for movements to targets located away from the body (targets 1-4) were higher compared to those located closer to the body (targets 5-8) by 18.4% (CI [17.4, 19.4], $p < 0.001$). Next, we found that the net coupling torque (calculated as the sum of absolute coupling torques at both joints) during control was correlated with the change in hand velocities during cerebellar block, particularly for targets located away from the body (targets 1-4: $\rho = 0.40$, CI [0.06, 0.69], $p = 0.020$; targets 5-8: $\rho = 0.28$, CI [-0.08, 0.59], $p = 0.096$). This indicated that the effect of the cerebellar block on target-specific hand velocity was strongest for movements to targets with high coupling torques.

Using the inverse dynamic model, we found that the reason for the target-specific reduction in velocities was a change in the muscle commands. Specifically, we found that muscle torque amplitude was reduced in a target and joint-specific manner during cerebellar block, leading to lower coupling torques (**Figure 1f**; **Supplementary table S3** and **S4a**). Furthermore, for targets 1-4, the shoulder joint experienced a significantly higher reduction in muscle torque than the elbow (shoulder: 18.4% reduction, CI [16.2, 20.5], $p < 0.001$; elbow: 10.8% reduction, CI [8.2, 13.4], $p < 0.001$). This may be attributed to the stronger role of the shoulder joint in generating coupling torques due to the larger inertial properties of the upper arm. Taken together we found that during cerebellar there is a reduction in muscle torque specifically for targets in directions in which interaction torques are highest, and this reduction leads to target-specific reduction in hand velocity.

Despite the significant correlation between the reduced velocity and coupling torques, we found that cerebellar block reduced hand velocity even in single joint movements (e.g., target 1) where the elbow joint was stationary (mean reduction: target 1 = 19.5%, CI [16.6, 22.6], $p < 0.001$, target 5 = 8.3%, CI [5.7, 11.0], $p < 0.001$, **Supplementary table S4b**). This finding highlights a reduction in the motor command which takes place in addition and beyond the effect of the poor prediction of coupling torques to targets in which the elbow was stationary. **Figure 1g** summarizes the target-dependent effect of cerebellar block on coupling and muscle torques, for each joint.

Finally, we asked if a uniform weakness across the shoulder and elbow joints could generate the observed target-specific effects of cerebellar block on the coupling torque. To this end, we simulated the effect of the cerebellar block as five distinct levels of uniform reduction of shoulder and elbow muscle torque (relative to control) across all movement directions (**Supplementary Figure S1a**). We then computed the coupling torques produced by the simulated muscle torques (**Supplementary Figure S1b**). Even though the percentage reduction of muscle torques was the same across all targets, the resultant change in coupling torques was non-uniform. Nonetheless, there was a discrepancy between the simulated muscle and coupling torques when assuming global weakness and the measured torques during cerebellar block, especially for targets away from the body (targets 2-4) where coupling torques are high.

Overall, cerebellar block produced a systematic target and joint-specific lowering of the muscle torques in a manner that was strongly correlated with the coupling torques. However, a reduction in muscle torques was also evident during single-joint movements demonstrating the existence of an added component of weakness which exacerbated the level of motor impairment in this condition.

Hand velocity exhibits an adaptive trend during repeated movements to the same target during cerebellar block.

The advantage of using a reversible cerebellar block in an animal model is the ability to track the temporal profile of the motor impairments induced in this condition and thus to distinguish between primary and compensatory effects. To this end we assessed changes in hand kinematics when two monkeys made repeated movements to the same target during control and cerebellar block. In this experiment we used only those targets that specifically required dual-joint movements (i.e., targets 2-4 and 6-8). We found that during the control condition, the peak hand velocity remained stable across repeated trials for movements to targets located both away and near the body. However, cerebellar block affected the hand velocity in a trial and target-dependent manner (**Figure 2a**) such that for targets away from the body, velocity of late trials 11-20 was significantly lower than that of early trials 1-2 (trial type × trial sequence interaction effect: $p = 0.033$, **Supplementary Table S5**). Furthermore, already during the early trials, the reduction of hand was target dependent, such that for movements to targets 2-4, the hand velocity started 5.5% (CI [2.7, 8.2], $p < 0.001$; **Figure 2b**) lower during cerebellar block whereas the same effect was not observed for movements to targets 5-8 ($p = 0.46$, **Figure 2c**).

Taken together these results reveal that the hand velocity of multi-joint movements during cerebellar block was already low initially, reflecting a primary weakness effect. Over and above this, there was a further progressive decline of the hand velocity during successive movements most likely due to an adaptive response to the inability to compensate for coupling torques. This effect was particularly noticeable for movements directed away from the body where coupling is particularly high.

The slow movements during cerebellar block cannot fully account for the impaired motor timing.

Individuals with cerebellar deficits suffer from poorly timed movements, such as asynchronous activation of joints during multi-joint movements leading to movement decomposition (16) or spatial

variability in their movement trajectories across trials (25). However, these properties of movement are also velocity-dependent (16, 26). Therefore, it is conceivable that the combination of primary weakness and the strategic reduction in velocity to reduce the effects of coupling torque observed in our results is the main driver to the abnormal motor timing. To test this, we examined movement decomposition and trajectory variability during the movements to targets 2-4 (which exhibited the highest reduction in hand velocity during cerebellar block) and measured the impact of hand velocity on these measures.

To quantify movement decomposition, we normalized the movement times of individual trials to range from 0 to 1 and identified the bins where either the shoulder or the elbow joint paused (angular velocity < 20°/s) while the other joint continued moving (16). In control trials, decomposition was primarily observed during the early phase of movement, where joint velocities are low making this measure more sensitive (**Figure 2d**). However, during cerebellar block trials, decomposition occurred throughout the movement (**Figure 2e**) To quantify this effect, we calculated a decomposition index for each trial, representing the proportion of movement time during which the movement was decomposed, as defined above. Overall, cerebellar block increased movement decomposition by 44.7% (CI [36.9, 53.4], $p < 0.001$). Next, we asked whether movement decomposition was mainly due to lower hand velocities. We therefore selected the subset of control trials that matched the cerebellar block trials in their peak velocities. However, movement decomposition in these control trials was only slightly higher (6.1%, CI [0.4, 11.9], $p = 0.029$) compared to all control trials and still 37.4% lower (CI [26.8, 49.1], $p < 0.001$) than the velocity-matched cerebellar block trials (**Figure 2f**). This indicates that even at matched velocities, movements made during cerebellar block were more decomposed than during control.

To assess trajectory variability, we first aligned the hand trajectories to have the same starting position, and then rotated them so that their endpoint was located on the positive Y-axis (**Figure 2g**). Subsequently, we defined the error of each trajectory as the maximal perpendicular distance from the Y-axis. The standard deviation of the errors across all trials was used to quantify the inter-trial trajectory variability. Normally, slower movements are also less variable due the speed-accuracy tradeoff (27). Therefore, we selected the subset of control trials that matched the cerebellar block trials in their peak velocities. Indeed, the trajectory variability in this subset of slower control trials was 9.8% (CI [4.8, 15.0], $p < 0.001$) lower than that of all control trials. However, when we compared the subset of velocity matched control and cerebellar block trials, we found that cerebellar block exhibited 19.7% (CI [11.9, 27.8], $p = 0.000$) higher trajectory variability (**Figure 2h)**. In other words, despite slower movements, cerebellar block increased trajectory variability.

Discussion

Cerebellar patients exhibit altered motor behavior related mostly to poor timing and coordination of voluntary movements. Understanding the impairments that follow cerebellar lesions is often complicated by the fact that the studies of this question mostly rely on a heterogeneous population of individuals with chronic cerebellar deficits due to different levels and types of cerebellar pathologies. Here we addressed this question by using high-frequency stimulation to reversibly block cerebellar output to the motor cortex in behaving monkeys wearing an exoskeleton (20) and comparing the post-block motor behavior to pre-block control conditions. Our results indicate that cerebellar block leads to decreased hand velocity via two mechanisms: a generalized reduction in muscle torques suggesting motor weakness, and spatially tuned decreases in velocity in targets where large inter-joint interactions occur, indicating a failure to compensate for limb dynamics. Analyzing the time course of these impairments reveal partially overlapping processes, with an This dual impact was evident as reduced initial reduction of hand velocity due to muscle weakness and a subsequent hand velocity in repeated movements to the same target under cerebellar block, which further decreased velocity over successive trials, in an apparent suggesting an adaptive strategy to minimize inter-joint interactions. Finally, we observed increased motor noise in terms of movement decomposition and inter-trial trajectory variability which were independent of the slower movements observed in cerebellar block.

Target dependent reduction in hand velocity and coupling torques during movements under cerebellar block.

Cerebellar block led to a target-specific reduction in hand velocity, even though the arm was fully supported by the exoskeleton and thus gravity did not play any role. This observation replicates findings made in previous studies that have documented slowing of movements in individuals with cerebellar lesions (28-30) as well as in monkeys which underwent dentate cooling (31). It was argued that the reduction in hand velocity may be a compensatory strategy to counteract the impaired ability to manage inter-joint coupling torques in the absence of cerebellar input to the motor cortex (16, 28, 32, 33). Since coupling torques in multi-joint movements are generated in a velocity-dependent manner (22, 34), slowing down the movement not only simplifies its kinetics (by reducing the impact of coupling torques) but also allows more time for slower visual feedback mechanisms to aid in guiding the movement (35). Our findings, which demonstrate a correlation between the extent of hand velocity reduction during cerebellar block and the magnitude of coupling torque under control conditions, further corroborate this hypothesis, and confirms our approach for reversible inactivation of cerebellar output as a model for ataxia. Furthermore, our model enabled us to study this effect rigorously and systematically while dissociating it from the other primary effects of cerebellar block as discussed below.

Muscle weakness is an acute response to cerebellar block.

Poor compensation of coupling torque has been a fundamental deficit in cerebellar ataxia (17). Nevertheless, several studies have argued that the inability to produce sufficient muscle torques may in fact be a primary deficit in cerebellar ataxia (29, 36-39). Since in most of these studies the upper limb was not fully supported during the task, it likely required maneuvering against gravity which may complicate the interpretation of the results. Here, although we removed the effect of gravity, we found a significant reduction in hand velocity and muscle torques due to cerebellar block during movements with a predominant involvement of a single-joint (shoulder flexion/extension), where coupling torques are negligible. Furthermore, we also showed that this weakness appears immediately after cerebellar block resulting in lower hand velocity in the first few test trials. This initial reduction in hand velocity was followed by an additional, gradual decline across the subsequent trials before reaching a stable value. We, therefore, conclude that the slower movements in the absence of cerebellar signals is likely an outcome of two main factors: first a primary inability to generate sufficient muscle torques and a secondary adaptive strategy aimed to compensate for impaired prediction of limb dynamics. Previous studies have reported upper limb weakness (loss of muscle tone), especially at the shoulder, in individuals with lesions at multiple locations of the cerebello-thalamo-cortical pathway, including the cerebellum (11, 13) and the premotor cortex (40, 41). Our findings about the weakness suggests that cerebellar output provides a strong drive to the motor cortex, beyond its role in motor timing and coordination (42-44). As such, cerebellar output can serve as a site for modulating neural activity and motor cortical excitability for the purpose of post-stroke recovery (45).

Asynchronous joint movements and motor variability is unaffected by the movement velocity in cerebellar block.

Abnormally high motor variability (25, 46, 47) and decomposition of multi-joint movements (16) are core deficits in cerebellar patients. We showed that the cerebellar block decomposed the dual-joint movements into temporally isolated single-joint actions and led to an increased trial-to-trial spatial noise. These two measures can be affected (in the opposite manner) by the reduction in movement velocities. Our results showed that even though movement decomposition increased with reduction in velocity in control trials, they were still significantly lower than that of velocity-matched cerebellar block trials. Second, the trial-to-trial spatial noise in hand trajectories increased during cerebellar block despite the slower movement speeds. The cerebellum is known to participate in the planning of movements by providing an internal model of the limb which is necessary for predicting the sensory outcomes of motor commands (4). For this purpose, the

cerebellum aids in estimating the state of the limb by integrating the sensory information of its last known state with predictions of its response to the latest motor command (48, 49). Therefore, in the absence of cerebellar signals, there are programming errors in the feedforward command required to launch the limb accurately towards a target (25). These feedforward errors may in turn translate into the noisy joint activation patterns and unpredictable hand trajectories observed in our results. Moreover, the persistence of these deficits independently of the movement speeds observed during cerebellar block indicates that they cannot be compensated for, unlike the impaired prediction of inter-joint interactions which are strategically dealt with by reducing the movement velocity.

In summary, our study demonstrated the presence of muscle weakness as a primary deficit in an acute model of cerebellar ataxia. Over and above this primary deficit, we observed a secondary slowing of movements most likely due to the inability to compensate for inter-joint interactions which arise in rapid, ballistic movements. This inability may be tied to a faulty internal model of feedforward control. Such feedforward errors also give rise to increased motor variability and asynchronous joint activations, which manifest even at the slow movement speeds observed during cerebellar block.

Materials and Methods

Experimental subjects

This study was performed on four adult female monkeys (*Macaca fascicularis*, weight 4.5-8 kg). The care and surgical procedures of the subjects will be in accordance with the Hebrew University Guidelines for the Use and Care of Laboratory Animals in Research, supervised by the Institutional Committee for Animal Care and Use.

Behavioral task

Each monkey was trained to sit in a primate chair and perform a planar, center-out reaching task. During the task, the left upper arm was abducted 90° and rested on cushioned troughs secured to links of a two-joint exoskeleton (KINARM, BKIN Technologies Ltd.). The sequence of events in each trial of this task was as follows. First, the monkey located a cursor (projected on a horizontal screen immediately above its arm) within a central target. After 500-800 ms, a randomly selected peripheral target (out of 8 evenly distributed targets) was displayed. The monkey had to wait until the central target disappeared (i.e., the ‘go’ signal) and then reach the cued peripheral target. This delay between the cue and the ‘go’ signal was 450-600 ms. The monkey was rewarded with a drop of applesauce if it moved the cursor to the correct target within 1 s of the ‘go’ signal.

Insertion of the stimulating electrode into the superior cerebellar peduncle

After the training was completed, a square recording chamber (24x24 mm) was attached to the monkey’s skull above the upper limb related area of the motor cortex in a surgical procedure under general anesthesia. To insert a chronic stimulating electrode into the ipsilateral superior cerebellar peduncle (SCP), a round chamber (diameter = 19 mm) was also implanted above the estimated insertion point (as per stereotactic measurements) during the surgery for the cortical chamber implantation. Subsequently, a post-surgery MRI was used to plan the trajectory for the electrode insertion into the SCP. After a recovery and re-training period, a bi-polar concentric electrode (Microprobes for Life Science Inc.) was inserted through the round chamber along the planned trajectory. During the process of insertion, the evoked multi-unit activity in the primary motor cortex was simultaneously monitored to identify the precise location where the stimulating electrode should be secured (42, 50).

High frequency stimulation to block the cerebellar outflow to the motor cortex

The superior cerebellar peduncle was blocked using high-frequency stimulation (20). This stimulation protocol consisted of a train of biphasic rectangular-pulse stimuli (where each phase was 200 µs) applied at 130 Hz. Each train was delivered at a fixed intensity of 150-250 µA.

Data collection protocol

Each monkey performed the experimental task for several days (sessions). Each session was divided into three or four sub-sessions. Each sub-session further comprised of blocks of control trials and trials with the superior cerebellar peduncle blocked using high-frequency stimulation as described above. During the task performance the following behavioral data was obtained at 1000 Hz using the KINARM's motor encoders: (i) Hand position in the x-y plane of movement, (ii) Elbow and shoulder joint angular positions, velocities, and accelerations. The lengths of the upper arm and forearm of each monkey were measured as the distances from the head of the humerus to the lateral epicondyle and from the lateral epicondyle to the palm respectively. The inertial properties of the upper limb were estimated using the monkey's body weight (51).

Processing of the behavioral data

All data analysis was performed in MATLAB R2021b (MathWorks Inc.). The raw kinematic data was low-passed filtered by using a second order Butterworth filter (cutoff = 10Hz) and then epoched into trials. For this purpose, the start and end events were taken as the time of presentation of the cue (i.e., the peripheral target) and the time of entry of the control cursor into the peripheral target respectively. The movement onset was defined as the time when the radial hand velocity exceeded 5% of its peak. Subsequently all the trials were zero-centered around the calculated movement onset. We then applied a two-links inverse dynamics model of the upper arm to the kinematic data to compute the coupling and muscle torques acting on the elbow and shoulder joints (24). The inverse dynamics equations of motion for the combined system consisting of the monkey's arm and the associated moving components of the KINARM were used to compute the joint torques:

$$T_{me} = T_{ne} - T_{ce} \quad \text{(i)}$$

$$T_{ms} = T_{ns} - T_{cs} \quad \text{(ii)}$$

where T_{ne} and T_{ns} are the net torques (proportional to the joint's acceleration), T_{ce} and T_{cs} are passive coupling torques, and T_{me} and T_{ms} are the active muscle torques acting at the elbow and shoulder joints respectively. The expanded formulas for computing each of the above terms are provided by equations 1a-2e in the methods section C of (24). It must be noted that the 'muscle' torques computed here include the effects of the actively generated muscle forces as well as the viscoelastic effects that result from the musculoskeletal system and the KINARM (52).

For the simulations conducted in this study, we used the muscle torques as inputs to forward dynamics equations. These were obtained by reformulating the inverse dynamics equations as a set of four first order differential equations representing the shoulder and elbow angular positions and velocities (53). These equations were then numerically integrated using a Runge-Kutta algorithm (ode89 in MATLAB). The joint accelerations were subsequently obtained by three-point numerical differentiation of the corresponding joint velocities. As an internal consistency check, we computed the joint kinematics using the calculated muscle torques to ensure that they are indistinguishable from the recorded kinematics.

Statistical analyses

We used linear mixed effects analysis for evaluating the effects of predictor variables of interest on the computed response variables. This allowed us to account for the variability across the monkeys which was modelled as a random effect. For *post-hoc* comparisons and confidence interval calculations of the group means, we used the bootstrap approach. In this approach, each

bootstrapped sample (n = 1000) was generated in the following manner. For each monkey, the original data was sampled with replacement for the variable of interest (e.g., peak hand velocity). Subsequently the test statistic was computed (e.g., percentage change of mean peak hand velocity in cerebellar block relative to control). This test statistic was then averaged across all the monkeys to generate the bootstrap sample. This allowed us to control the different number of samples/trials available per condition per monkey. The p-value was then computed by comparing the observed test statistic to the bootstrapped distribution of the test statistic as calculated above (54). The computed p-values were then corrected using the Benjamini-Hochberg procedure to control the false discovery rate for multiple *post-hoc* comparisons, wherever applicable (55). A significance level of 0.05 was used for all comparisons in this study.

Acknowledgments

This work was funded by the Israel Science Foundation (ISF-1801/18 and ISF 1207/23) to Y.P., the Deutsche Forschungsgemeinschaft (DFG, German Research Foundation Project-ID 431549029–SFB 1451) to Y.P., the National Institutes of Health (NIH R01NS105759) to J.P.A.D., the Council for Higher Education PhD Sandwich Fellowship, Government of Israel to N.S., and the generous support of the Baruch Foundation to Y.P. The authors would like to thank Dr. Abdulraheem Nashef, post-doctoral fellow at the University of Colorado for collecting part of the data used in this study.

References

1. H. Beppu, M. Suda, R. Tanaka, ANALYSIS OF CEREBELLAR MOTOR DISORDERS BY VISUALLY GUIDED ELBOW TRACKING MOVEMENT. *Brain* **107**, 787-809 (1984).
2. M. Manto *et al.*, Consensus Paper: Roles of the Cerebellum in Motor Control-The Diversity of Ideas on Cerebellar Involvement in Movement. *Cerebellum (London, England)* **11**, 457-487 (2011).
3. R. B. Ivry, S. W. Keele, Timing Functions of The Cerebellum. *Journal of Cognitive Neuroscience* **1**, 136-152 (1989).
4. D. M. Wolpert, R. C. Miall, M. Kawato, Internal models in the cerebellum. *Trends Cogn. Sci. (Regul. Ed.)* **2**, 338-347 (1998).
5. M. Kawato, Internal models for motor control and trajectory planning. *Current Opinion in Neurobiology* **9**, 718-727 (1999).
6. M. Shidara, K. Kawano, H. Gomi, M. Kawato, Inverse-dynamics model eye movement control by Purkinje cells in the cerebellum. *Nature* **365**, 50-52 (1993).
7. L. Popa, A. Hewitt, T. Ebner, Purkinje Cell Simple Spike Discharge Encodes Error Signals Consistent with a Forward Internal Model. *Cerebellum (London, England)* **12** (2013).
8. R. Shadmehr, F. Mussa-Ivaldi, Adaptive representation of dynamics during learning of a motor task. *The Journal of Neuroscience* **14**, 3208-3224 (1994).
9. R. L. Sainburg, C. Ghez, D. Kalakanis, Intersegmental Dynamics Are Controlled by Sequential Anticipatory, Error Correction, and Postural Mechanisms. *J. Neurophysiol.* **81**, 1045-1056 (1999).
10. D. M. Wolpert, Z. Ghahramani, M. I. Jordan, An Internal Model for Sensorimotor Integration. *Science* **269**, 1880-1882 (1995).
11. G. Holmes, THE CEREBELLUM OF MAN1. *Brain* **62**, 1-30 (1939).
12. K. Goldstein, Das Kleinhirn. *Handbuch der normalen und pathologischen Physiologie* **10**, 222-222 (1927).
13. G. Holmes, The symptoms of acute cerebellar injuries due to gunshot injuries. *Brain: A Journal of Neurology* **40**, 461-535 (1917).
14. D. J. Szmulewicz *et al.*, Sensory neuropathy as part of the cerebellar ataxia neuropathy vestibular areflexia syndrome. *Neurology* **76**, 1903-1910 (2011).
15. H. M. Weeks, A. S. Therrien, A. J. Bastian, Proprioceptive Localization Deficits in People With Cerebellar Damage. *The Cerebellum* **16**, 427-437 (2017).

16. A. J. Bastian, T. A. Martin, J. G. Keating, W. T. Thach, Cerebellar ataxia: abnormal control of interaction torques across multiple joints. *J. Neurophysiol.* **76**, 492-509 (1996).
17. A. J. Bastian, K. M. Zackowski, W. T. Thach, Cerebellar Ataxia: Torque Deficiency or Torque Mismatch Between Joints? *J. Neurophysiol.* **83**, 3019-3030 (2000).
18. H. Topka, J. Konczak, K. Schneider, A. Boose, J. Dichgans, Multijoint arm movements in cerebellar ataxia: Abnormal control of movement dynamics. *Exp Brain Res* **119**, 493-503 (1998).
19. A. Boose, J. Dichgans, H. Topka, Deficits in phasic muscle force generation explain insufficient compensation for interaction torque in cerebellar patients. *Neuroscience Letters* **261**, 53-56 (1999).
20. A. Nashef, O. Cohen, R. Harel, Z. Israel, Y. Prut, Reversible Block of Cerebellar Outflow Reveals Cortical Circuitry for Motor Coordination. *Cell Rep* **27**, 2608-2619.e2604 (2019).
21. S. H. Scott, Optimal feedback control and the neural basis of volitional motor control. *Nature Reviews Neuroscience* **5**, 532-545 (2004).
22. J. M. Hollerbach, T. Flash, Dynamic interactions between limb segments during planar arm movement. *Biological Cybernetics* **44**, 67-77 (1982).
23. N. A. Bernshteĭn (1967) The co-ordination and regulation of movements. (Pergamon Press Oxford, Oxford).
24. A. Fagg, G. Ojakangas, L. Miller, N. Hatsopoulos, Kinetic Trajectory Decoding Using Motor Cortical Ensembles. *IEEE transactions on neural systems and rehabilitation engineering : a publication of the IEEE Engineering in Medicine and Biology Society* **17**, 487-496 (2009).
25. B. L. Day, P. D. Thompson, A. E. Harding, C. D. Marsden, Influence of vision on upper limb reaching movements in patients with cerebellar ataxia. *Brain* **121**, 357-372 (1998).
26. R. Osu, K.-i. Morishige, J. Nakanishi, H. Miyamoto, M. Kawato, Practice reduces task relevant variance modulation and forms nominal trajectory. *Scientific Reports* **5**, 17659 (2015).
27. R. Plamondon, A. M. Alimi, Speed/accuracy trade-offs in target-directed movements. *Behavioral and Brain Sciences* **20**, 279-303 (1997).
28. B. Wild, J. Dichgans, Cerebellar ataxia in ataxic hemiparesis? A kinematic and EMG analysis. *Movement Disorders* **8**, 363-366 (1993).
29. H. Topka, J. Konczak, J. Dichgans, Coordination of multi-joint arm movements in cerebellar ataxia:Analysis of hand and angular kinematics. *Exp Brain Res* **119**, 483-492 (1998).
30. J. Konczak, B. Schoch, A. Dimitrova, E. Gizewski, D. Timmann, Functional recovery of children and adolescents after cerebellar tumour resection. *Brain* **128**, 1428-1441 (2005).
31. T. Tsujimoto, H. Gemba, K. Sasaki, Effect of cooling the dentate nucleus of the cerebellum on hand movement of the monkey. *Brain Research* **629**, 1-9 (1993).
32. A. J. Bastian, W. T. Thach, Cerebellar outflow lesions: A comparison of movement deficits resulting from lesions at the levels of the cerebellum and thalamus. *Annals of Neurology* **38**, 881-892 (1995).
33. R. F. Beer, J. P. A. Dewald, W. Z. Rymer, Deficits in the coordination of multijoint arm movements in patients with hemiparesis: evidence for disturbed control of limb dynamics. *Exp Brain Res* **131**, 305-319 (2000).
34. N. Virji-Babul, J. D. Cooke, Influence of joint interactional effects on the coordination of planar two-joint arm movements. *Exp Brain Res* **103**, 451-459 (1995).
35. M. Jeannerod, *The neural and behavioural organization of goal-directed movements*, The neural and behavioural organization of goal-directed movements. (Clarendon Press/Oxford University Press, New York, NY, US, 1988), pp. xii, 283-xii, 283.
36. M. Hallett, S. Massaquoi, Kinematics of Initiating a Two-Joint Arm Movement in Patients with Cerebellar Ataxia. *Canadian Journal of Neurological Sciences / Journal Canadien des Sciences Neurologiques* **23**, 3-14 (1996).
37. J. Hore, B. Wild, H. C. Diener, Cerebellar dysmetria at the elbow, wrist, and fingers. *J. Neurophysiol.* **65**, 563-571 (1991).

38. B. Wild, T. Klockgether, J. Dichgans, Acceleration deficit in patients with cerebellar lesions. A study of kinematic and EMG-parameters in fast wrist movements. *Brain Research* **713**, 186-191 (1996).
39. H. Mark, G. M. Steve, Physiologic Studies of Dysmetria in Patients with Cerebellar Deficits. *Canadian Journal of Neurological Sciences / Journal Canadien des Sciences Neurologiques* **20**, S83-S92 (1993).
40. H.-J. Freund, Clinical aspects of premotor function. *Behavioural Brain Research* **18**, 187-191 (1985).
41. H. J. Freund, H. Hummelsheim, Lesions of premotor cortex in man. *Brain : a journal of neurology* **108 (Pt 3)**, 697-733 (1985).
42. A. Nashef, O. Cohen, Z. Israel, R. Harel, Y. Prut, Cerebellar Shaping of Motor Cortical Firing Is Correlated with Timing of Motor Actions. *Cell Rep* **23**, 1275-1285 (2018).
43. Y. Shinoda, M. Yamazaki, T. Futami, Convergent inputs from the dentate and the interpositus nuclei to pyramidal tract neurons in the motor cortex. *Neuroscience Letters* **34**, 111-115 (1982).
44. J. Hore, D. Flament, Changes in motor cortex neural discharge associated with the development of cerebellar limb ataxia. *J. Neurophysiol.* **60**, 1285-1302 (1988).
45. K. B. Baker *et al.*, Cerebellar deep brain stimulation for chronic post-stroke motor rehabilitation: a phase I trial. *Nature Medicine* **29**, 2366-2374 (2023).
46. D. Timmann, S. Watts, J. Hore, Failure of Cerebellar Patients to Time Finger Opening Precisely Causes Ball High-Low Inaccuracy in Overarm Throws. *J. Neurophysiol.* **82**, 103-114 (1999).
47. J. E. Schlerf, J. Xu, N. M. Klemfuss, T. L. Griffiths, R. B. Ivry, Individuals with cerebellar degeneration show similar adaptation deficits with large and small visuomotor errors. *J. Neurophysiol.* **109**, 1164-1173 (2012).
48. R. C. Miall, L. O. D. Christensen, O. Cain, J. Stanley, Disruption of State Estimation in the Human Lateral Cerebellum. *PLOS Biology* **5**, e316 (2007).
49. R. C. Miall, D. King, State Estimation in the Cerebellum. *The Cerebellum* **7**, 572-576 (2008).
50. A. Nashef, H. Rapp, M. P. Nawrot, Y. Prut, Area-specific processing of cerebellar-thalamo-cortical information in primates. *Biological Cybernetics* **112**, 141-152 (2018).
51. E. J. Cheng, S. H. Scott, Morphometry of Macaca mulatta forelimb. I. Shoulder and elbow muscles and segment inertial parameters. *Journal of Morphology* **245**, 206-224 (2000).
52. J. L. Smith, R. F. Zernicke, Predictions for neural control based on limb dynamics. *Trends Neurosci* **10**, 123-128 (1987).
53. C. M. Close, D. K. Frederick, J. C. Newell, *Modeling and analysis of dynamic systems* (John Wiley & Sons, 2001).
54. A. C. Davison, D. V. Hinkley, *Bootstrap Methods and their Application*, Cambridge Series in Statistical and Probabilistic Mathematics (Cambridge University Press, Cambridge, 1997), DOI: 10.1017/CBO9780511802843.
55. W. Haynes, "Benjamini–Hochberg Method" in Encyclopedia of Systems Biology, W. Dubitzky, O. Wolkenhauer, K.-H. Cho, H. Yokota, Eds. (Springer New York, New York, NY, 2013), 10.1007/978-1-4419-9863-7_1215, pp. 78-78.

Figures and Tables

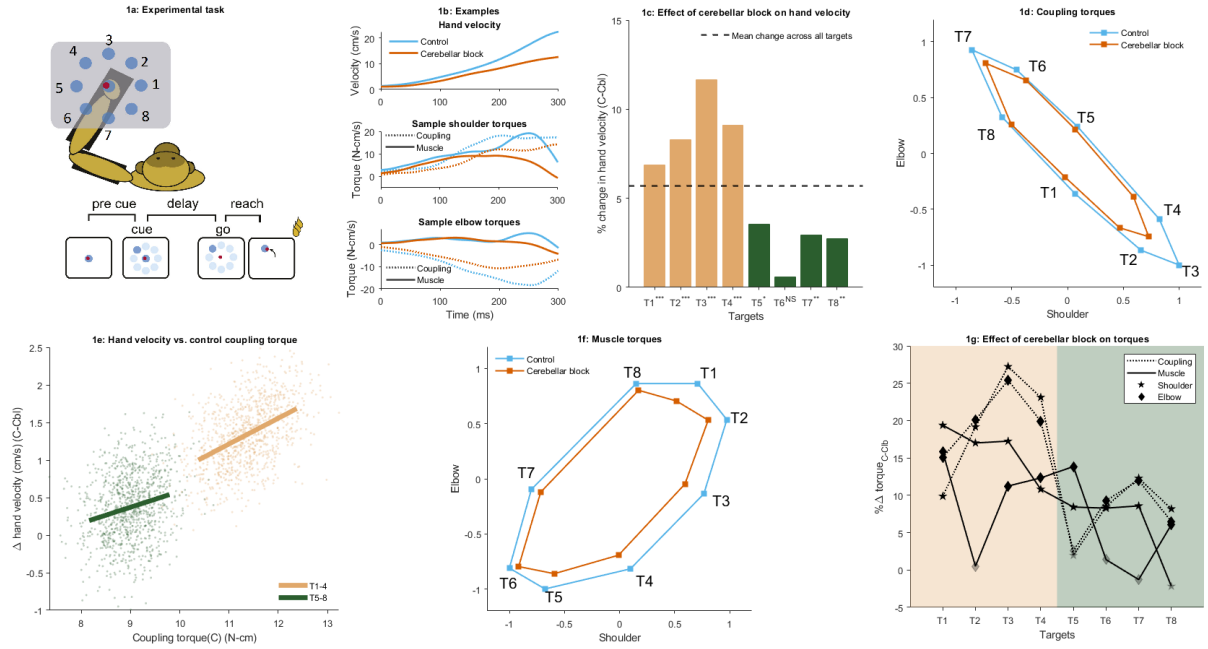

Figure 1: Effect of cerebellar block on hand velocities and joint torques. (a) Schematic of the monkey performing the delayed reaching task in the KINARM exoskeleton to eight peripheral targets on the horizontal plane. The locations of the eight targets are numbered. (b) From top to bottom: hand velocity, shoulder and elbow torque traces for a sample control and cerebellar block trials performed by monkey C to target 3. (c) Target-wise effect of cerebellar block on peak hand velocity. The change in peak hand velocity was computed relative to the maximum peak hand velocity in control across all targets. $p \geq 0.05^{NS}$, $p < 0.05$*, $p < 0.01$**, $p < 0.001$***. (d) Normalized mean absolute coupling torque at shoulder vs. elbow joint per target in control and cerebellar block. The torques at each joint were normalized by the maximum torque for that joint across all targets. (e) Difference in hand velocity (control-cerebellar block) plotted against the mean absolute coupling torque in control. The lines overlayed on the scatters indicate the least-squares linear regression fits to the data points of each group. (f) Normalized mean absolute muscle torque at shoulder vs. elbow per target direction in control and cerebellar block. The torques at each joint were normalized by the maximum torque for that joint across all targets. (g) Reduction of mean absolute coupling and muscle torques at each joint due to cerebellar block as a percentage of the corresponding maximum torque in control for that joint across all targets. Bold markers denote significant effect ($p < 0.05$). Color coding for target groups (1-4 vs. 5-8) same as in (c). [C: Control, Cbl: Cerebellar block; T1-8: Targets 1-8]

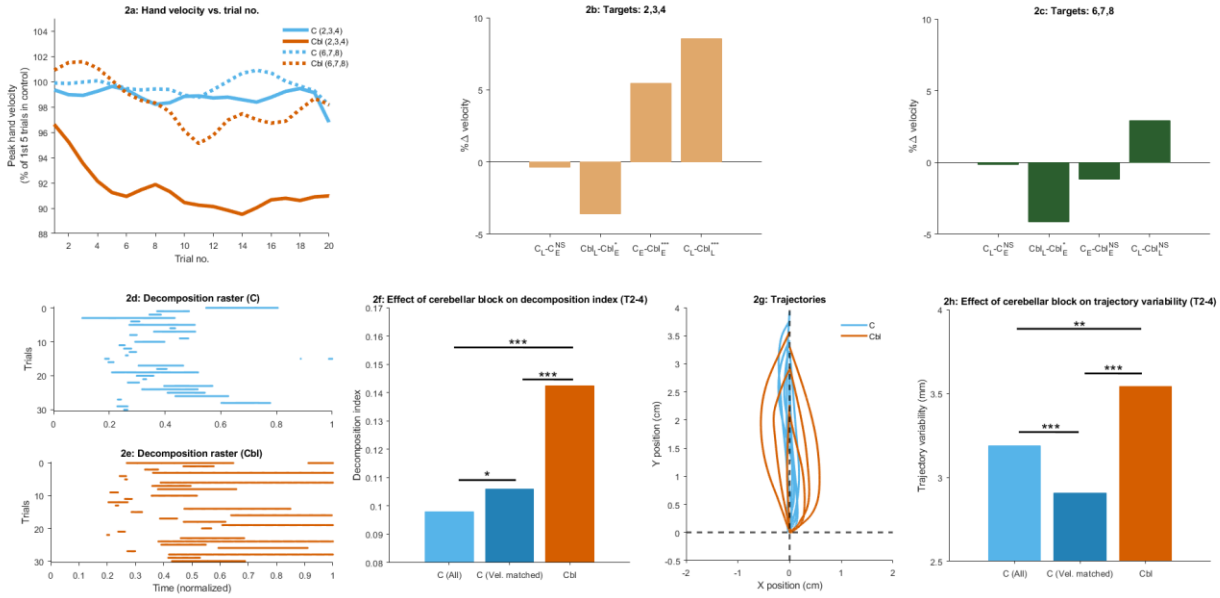

Figure 2a-c: Effect of the cerebellar block on hand velocity across successive trials. (a) Peak hand velocity across successive trials when repeated movements were made to the same target. Data was pooled into two groups: movements to the forward targets 2-4 and backward targets 6-8. (b) Bar plots showing mean percentage change of hand velocity for targets 2-4 between (i) early (trial no. 1-2) vs. late (trial no. 11-20) control trials, (ii) early vs. late cerebellar block trials, (iii) early cerebellar block vs. early control trials and (iv) late cerebellar block vs. late control trials. (c) Same as in (b) but for targets 6-8. **Figure 2d-f: Effect of the cerebellar block on the decomposition of dual-joint movements.** (d) Binary decomposition raster of sample trials for movements made to target 3 by monkey S during control. The duration of each trial was normalized to 0-1 (0.001 bin width) and then decomposition was computed for each bin based on whether either (but not both) of the shoulder or the elbow joint velocity was less than 20°/s. (e) Same as in (d) but for movements to target 3 by monkey S during cerebellar block. (f) Mean decomposition index (i.e., the proportion of the movement time during which the movement was decomposed, as defined above) for movements to targets 2-4 during all control trials and velocity matched control vs. cerebellar block trials. **Figure 2g-h: Effect of the cerebellar block on inter-trial trajectory variability.** (g) Sample hand trajectories during control vs. cerebellar block trials for movements to target 3 by monkey S. The starting point of the trajectories was shifted to the origin and then they were rotated about the origin so that their endpoints lie on the positive Y-axis. (h) Mean inter-trial trajectory variability as measured by the standard deviation of the maximum distance of the trajectories from the Y-axis after transforming them as in (g). The trajectory variability was computed for movements to targets 2-4 during all control trials and velocity matched control vs. cerebellar block trials. [C: Control, Cbl: Cerebellar block; T1-8: Targets 1-8, $p \geq 0.05^{NS}$, $p < 0.05$*, $p < 0.01$**, $p < 0.001$***]